Molecular dynamics of polymer growth

Reinier L. C. Akkermans, So/ren Toxvaerd, and W. J. Briels

Citation: The Journal of Chemical Physics **109**, 2929 (1998); doi: 10.1063/1.476845
View online: http://dx.doi.org/10.1063/1.476845
View Table of Contents: http://scitation.aip.org/content/aip/journal/jcp/109/7?ver=pdfcov
Published by the AIP Publishing

Molecular dynamics of polymer growth

Reinier L. C. Akkermans
Laboratory of Chemical Physics, University of Twente, P.O. Box 217, 7500 AE Enschede, The Netherlands

Søren Toxvaerd
Department of Chemistry, H. C. Ørsted Institute, University of Copenhagen, DK–2100 Copenhagen Ø, Denmark

W. J. Briels
Laboratory of Chemical Physics, University of Twente, P.O. Box 217, 7500 AE Enschede, The Netherlands

(Received 6 January 1998; accepted 14 May 1998)

The irreversible polymerization of a monomer liquid has been studied by molecular-dynamics simulation in two and three dimensions. The growth process is studied under good solvent conditions in the dilute regime and up to semidilute and concentrated regimes. In the dilute regime we observe a reaction limitation due to trapping of the growing centers, which is more pronounced in the lower dimension. At higher concentrations the presence of other chains decreases the monomer mobility and reaction rate. Conformational properties are studied by scaling analysis of end-to-end and gyration radii. A crossover from swollen conformations towards screened conformations is observed as growth proceeds. © *1998 American Institute of Physics.* [S0021-9606(98)51231-7]

I. INTRODUCTION

Relaxation times of molecular systems easily exceed those covered by molecular dynamics (MD) simulations when the size of the molecules increases. In particular, for simple linear polymers, the relaxation of the end-to-end distance scales as N^2 with the polymer length, according to Rouse theory. Clearly, if one wants to calculate configurational properties of such systems from MD simulation, a large number of simulations starting from different initial structures have to be performed to sample a sufficient part of the configuration space. It is then important to have a method available that generates initial states from the expected equilibrium distribution.

An effective method will generate structures that satisfy at least two criteria: (i) The chains have correct conformational statistics and (ii) the polymer segments are homogeneously distributed. A number of methods for generating equilibrium polymer samples have been proposed[1–10] starting from either one of the two criteria.

The technique most widely used in generating amorphous polymer melt structures is to generate chains in vacuum satisfying the expected conformational statistics for the melt and to pack these into a periodic box at the required density.[1] The conformational statistics in the melt are simplified by Flory's hypothesis,[11] stating that the intrachain excluded volume interactions in the melt just offset the interchain interactions. This allows one to generate single polymer configurations in accordance with those in a melt, by taking only local interactions into account, for example using the rotational isomeric state model[11] or, similarly, by equilibrating a single chain with a localized Hamiltonian (pivot Monte Carlo[2]). The major problem in this approach is how to pack the chains into a periodic box; that is, how to account for the supposedly screened interactions. By simply packing the chains at the final densities one reaches a state with severe overlap and straightforward equilibration using the full Hamiltonian is prohibited. Instead, energy minimization is often used to reach a state with reasonable potential energy, but this may affect the conformational statistics and does not guarantee a homogeneous system. It has been found that the packing is conveniently carried out using a modified, purely repulsive, Hamiltonian combined with isobaric simulation with low coupling to a high-pressure bath starting from a rarefied system.[12,13]

Another approach is to start from a homogeneous distribution of monomers and to introduce the bonded interactions in a separate step.[4–10] This can be thought of as an *in situ* polymerization. Here, it is important to have a polymerization process that yields chains with a conformation distribution that is expected at the concentration of interest. It has the advantage that polymer systems of arbitrary dilution can easily be generated. Moreover, the method can also be applied to two-dimensional (2D) systems, which is not straightforward with the first method, because of severe restrictions caused by repulsive interactions in two dimensions. This growing process is the target of this study.

Apart from being of interest as a tool in the simulation of polymer solutions, the very process of polymer growth is an interesting and challenging subject to simulation science. MD methods are becoming increasingly useful in studying dynamical processes involving chemical reactions, for example the phase separation in reactive binary mixtures,[14] and can be useful in understanding polymerization processes. For example, a molecular scale simulation can reveal the importance of the trapping of growth centers, the evolution of molecular weight distributions, conformational statistics during growth and explain how the polymerization product is related to processing history. In this work we develop a simple

dynamic model for addition polymerization of a model liquid, where monomers stick irreversibly and no termination of growing centers takes place, a situation similar to living polymers.

As we focus on simulating a polymerization process and are also interested in intermediate states, our work differs from the previous studies.[4–10] These are concerned with developing efficient algorithms that generate monodisperse polymer melt structures. In most studies the chains are generated statically. In order to connect all the monomers, the reaction radius has to be large and the generated structure is generally one of high potential energy. Consequently, energy minimization has to be performed to relax the generated structure. For example, Khare *et al.*[5] developed a method connecting monomers on a lattice in such a way that the shortest possible chain is obtained. Chains that did not satisfy the expected (experimental) end-to-end distance were rejected. Gao[6] connects ~70% of the monomers statically and uses simultaneous equilibration and growth with a larger reaction radius to connect the remaining monomers. In this last stage the spring constant is reduced to prevent the difficulty of very large bond forces. Kolinski *et al.*[7] developed a lattice Monte Carlo method for growth and equilibration of polymer chains, which was generalized for a continuum by Gupta *et al.*[9] They also included rotation barriers and found that due to the lack of internal rotations the method could only be applied to rather short chains (fewer than 25 segments). Finally, Lin *et al.*[10] used a growth and equilibration method to polymerize dimethyl ether to form polyethylene oxide. They also studied two different growth rates and found that the structure factor of the rapidly grown chains differs considerably from the one of the slowly grown chain, in particular for small scattering vectors, indicating that the large scale structure is not uniquely represented.

In this study we simulate the polymerization process in itself, without introducing any artificial changes in the growth mechanism with the sole purpose of speeding up the structure generation. We consider several reaction rates and compare the results with kinetic rate equations.

Lattice formulations have become a standard tool to study irreversible growth.[15–17] Here a ''walker'' travels on a lattice according to some given rule leaving a ''polymer'' as its trail. Clearly one can invent a variety of growth rules, e.g., random walk, self-avoiding walk, kinetic growth walk, etc., and each rule represents a different growth model. The only moving part in these formulations is the walker; the monomers (i.e., the lattice sites) have zero mobility and also the structure generated is frozen and not changing during the polymerization. As a consequence the ''trapping problem,'' i.e., the walker being surrounded by its own trail, is inherent to lattice formulations. It is then important to have a growth rule that avoids such situations.

Another approach in a related field is that of diffusion limited aggregation.[18] Here particles perform Brownian motion and stick irreversibly if they come close to each other thereby building a cluster. These models have the advantage of being easily simulated on a lattice, but loose their simplicity when one wants to account for diffusion (translation and rotation) of the cluster or restructuring of the cluster during the aggregation process. This is, for example, important if shear forces are present. A Brownian dynamics simulation of the diffusion-controlled growth of two-dimensional rodlike polymers under shear in which these effects are taken into account has been reported[19] but neglecting excluded-volume interactions. The MD method used in this study has the advantage that it is off-lattice and all motions (i.e., restructuring and diffusion) are implicitly taken into account while using a force field that includes excluded-volume interactions in a realistic manner.

The present study covers both two- and three-dimensional (3D) systems. Although chains in two and three dimensions share the properties of a connected object, their topologies differ in many aspects. In two dimensions steric hindrance is dramatic since a linear object behaves as a frontier in a plane, whereas in three dimensions it is essentially the finite system volume that causes steric effects. Moreover one cannot speak of entanglements in two dimensions. In a polymer melt the interaction between two monomers in a chain is screened by the presence of all the other chains, in both two and three dimensions. In two dimensions this means that the volume of the coil is proportional to the chain length; that is, the concentration inside the coil does not depend on the chain length, which is similar to the collapsed state of a two-dimensional chain in solution.[20,21] In three dimensions the melt conformations correspond to the theta-state of a chain in solution.

The use of two-dimensional systems is motivated by an increasing amount of experimental data on 2D polymerization processes.[22–25] Diffusion and trapping phenomena are found important in the description of reaction kinetics.[22,26] As simulating two-dimensional systems is generally less time consuming than 3D systems, these systems have been extensively studied.[18,21,27,28] Theoretically they have the advantage that some problems can be treated analytically, and that the differences in scaling regimes are more pronounced.

In the following section we describe the simulation and growth model. Equilibrium properties of a single chain in solution were investigated and are reported in Sec. III. In Sec. IV we discuss the growth model and report the single chain properties obtained from the growth simulations. Results on simultaneous growth of several chains towards concentrated solutions and melts are given in Sec. V. Discussion of these three sections is presented in the last section together with the conclusions.

II. MODEL AND SIMULATION DETAILS

Polymer growth is characterized by obeying universality laws, which indicates that details of the potential energies are unimportant and that orders of magnitude just set the units of time, density, and temperature. Although polymerization reactions are usually exothermic we believe that this is more an obstacle from a simulation point of view, than something that determines the physical chemistry of the product. Thus when simulating polymer growth by MD one has to concentrate on having a correct dynamics rather than simulating a certain polymerization. Also, the reaction time scale of a realistic polymerization looks to be prohibitive for MD when having in mind that MD only covers time intervals of the

order nano seconds, which means that one necessarily must ensure very fast kinetics with a low reaction barrier.

The polymerization is performed by creating covalent bonds between monomer units. Doing so we may introduce forces into the MD which are no longer given by a specific Hamiltonian. As a rule for the kinetics in the open MD system one should not introduce larger forces than the system is already exposed to especially during a high energy collision.[14] There is, however, a simple method to perform fast kinetics and polymerization by MD without introducing large forces and heat of reactions, which is used in the present study and described below.

In a condensed melt of monomers or polymers the mass units are confined in cages of nearest-neighbor mass units from which they escape occasionally. Thus they perform vibrations by colliding with their surroundings, determined in our case by the repulsive part of the Lennard-Jones (LJ) potential

$$u_{\mathrm{LJ}}(r)/\epsilon=\begin{cases}4((\sigma/r)^{12}-(\sigma/r)^{6})+1, & 0<r<r_m\\ 0, & r\geqslant r_m\end{cases}, \qquad (1)$$

where $r_m=2^{1/6}\sigma$.

The polymerization step is effected by not allowing a reacting monomer to escape simply by binding it on return from a collision. In order to ensure a smooth and symmetric bond potential u_b we reflect the LJ potential at its minimum r_m

$$u_b(r)=u_{\mathrm{LJ}}(r_m-|r-r_m|), \quad 0<r<2r_m. \qquad (2)$$

This bond potential is anharmonic and allows for a finite extensibility of the bonds of $2r_m$ with an equilibrium distance of r_m. It does not involve parameters other than the LJ parameters. We note that this spring-model is much weaker and the equilibrium distance is much larger than of a typical covalent bond. However, regarding the universal properties of polymers, the differences in spring-model only show up in prefactors and do not affect scaling properties. The local structure is kept simple (no higher order interactions, such as bond or torsion angles) in order to have a small persistence length such that scaling properties show up for comparably short chains. By using a bond potential similar to that of nonbonded interaction we bring the time scale of vibrational motion in correspondence with that for translational motion, and hence it allows us to use the same time step for a typical LJ liquid in simulating polymers. Furthermore we ensure that while the establishing the covalent bonds changes in the pressure are kept to a minimum, as a dimer has almost the same volume as two monomers in a liquid.

In the following we will distinguish between three types of particles: We will denote free monomers (or solvent molecules) by M and bonded monomers (or beads) by P. The bead at the chain end which acts as growth center is indicated by P^*. A polymer chain of n beads (or, n-mer) is denoted by P_n.

The reaction between growth centers and free monomers to give bonded monomers

$$M+P^*\rightarrow P^*-P,$$

$$M+P^*-P_n\rightarrow P^*-P_{n+1}, \quad n=1,2,\ldots,$$

is implemented by occasionally binding (M,P^*)-pairs on a high-energy collision. This includes all (M,P^*)-pairs that are separated by less than an encounter distance r_c. As in our model there is no difference between bonded and nonbonded interactions for $r\leqslant r_m$, we have set $r_c=r_m$ to have high reaction rate and no introduction of discontinuities in the forces or energy on reaction. Each time interval τ_r a reaction trial is performed by collecting all reactants of each growing center in the system. With m being the number of free monomers within a distance r_m from a growth center, we bind a random monomer with a probability $m/m_{\max}$, where $m_{\max}$ is a preset value, which should always be larger than m. From simulations of pure monomer liquid in three dimensions at the state point under investigation we know that the probability of finding more than eight monomers within a distance r_m around a given monomer is negligible, hence we have set $m_{\max}=8$, in both two and three dimensions. The reaction probability defined in this way accounts for the fact that the reaction rate of the bimolecular reaction is proportional to the local free monomer concentration.

We can thus write the average decrease in free monomer concentration as

$$[M(t+\tau_r)]-[M(t)]=-[P^*]\frac{\langle m\rangle}{m_{\max}}\approx\tau_r\frac{d[M]}{dt}, \qquad (3)$$

where $[\cdots]$ stands for number density (or concentration) and $[P^*]$ is the concentration of growth centers in the system. The average number of monomers around a growth center within the distance r_m, $\langle m\rangle$, can be expressed in terms of the radial distribution function of (M,P^*)-pairs

$$\langle m\rangle\approx[M]\int g_{MP^*}(r)d\boldsymbol{r}$$

$$=[M]\frac{2\pi^{d/2}}{\Gamma(d/2)}\int_0^{r_m}g_{MP^*}(r)r^{d-1}dr, \qquad (4)$$

where we have integrated over the angles in d-dimensions. In the following we use the expression for the three-dimensional case. For short chains the distribution function $g_{MP^*}(r)$ depends on the chain length but the integral converges rapidly to a constant value as the chain length increases. We shall use this value in the following and assume that the time dependence of $\langle m\rangle$ stems from $[M]$ only, and not from the structure.

By combining Eqs. (4) and (3) we obtain an expression for the consumption rate of free monomers in terms of the model parameters

$$\frac{d[M]}{dt}=-\frac{\int_0^{r_m}g_{MP^*}(r)4\pi r^2dr}{\tau_r m_{\max}}[M][P^*]. \qquad (5)$$

In our model growth centers cannot be destroyed; that is, we do not allow two chains to combine by binding their growth centers, nor do we allow disproportionation, where two growth centers saturate leaving two chains. As a consequence the number of growth centers and thus of chains is conserved during the simulation. We will also ignore all kinds of transfer reactions, where the growth center is transferred to other molecules. Furthermore, we assume the ini-

tiation step to be sufficiently fast, or unimportant, such that all the growth centers are present from the very beginning. These are conditions similar to preparation of living polymers.[29]

The kinetic equations for a sequence of reactions that does not involve destruction of the reactive species are given by[30,31]

$$\begin{cases} \dfrac{d[P_1]}{dt} = -k[M][P_1] \\ \dfrac{d[P_{n+1}]}{dt} = -k[M]([P_{n+1}]-[P_n]), \quad n=1,2,\ldots, \end{cases} \tag{6}$$

$$\frac{d[M]}{dt} = -k[M]\sum_{n=1}^{\infty}[P_n], \tag{7}$$

where $[P_n]$ is the concentration of n-mers, which is zero initially except for $[P_1(0)]\equiv[P^*]$. k denotes the reaction rate coefficient for the bimolecular reaction, which we assume independent of n. Consequently it is assumed that the reactants are ideally mixed and that diffusion is not important.

From Eq. (6) it is clear that the total number of reactive molecules is conserved, $\Sigma_{n=1}^{\infty}[P_n(t)]=[P^*]$. Using this in the expression for the monomer consumption [Eq. (7)], we obtain

$$\frac{[M(t)]}{[M]_0} = \exp(-k[P^*]t) \tag{8}$$

with initial condition $[M(0)]=[M]_0$. In other words, the free monomer concentration decreases exponentially to zero, as long as diffusion plays no role. To solve Eq. (6) it is useful to introduce the average number of bonds $N(t)$

$$N(t) = \frac{[M]_0-[M(t)]}{[P^*]} \tag{9}$$

$$= \frac{[M]_0}{[P^*]}(1-\exp(-k[P^*]t)) \tag{10}$$

$$= k\int_0^t [M(\tau)]d\tau, \tag{11}$$

which shows that the chain length increases linearly for small t, $N(t)\sim k[M]_0 t$, and then levels off asymptotically to $[M]_0/[P^*]$, the case where all monomer is consumed.

Equation (6) can be solved for $[P_n(t)]$ by substituting (11) in differential form, $dN=k[M]dt$. This leaves a Poisson distribution of n-mers,

$$\begin{cases} \dfrac{[P_1(t)]}{[P^*]} = \exp(-N(t)) \\ \dfrac{[P_{n+1}(t)]}{[P^*]} = \dfrac{N(t)^n}{n!}\exp(-N(t)), \quad n=1,2,\ldots. \end{cases} \tag{12}$$

The reaction rate coefficient k can be estimated by comparing Eqs. (5) and (7). If we assume that the integral over $g_{MP*}(r)$ is constant this yields

$$k = \frac{\int_0^{r_m} g_{MP*}(r)4\pi r^2 dr}{\tau_r m_{\max}}. \tag{13}$$

Using this value for k we will compare the macroscopic equations with our simulation results.

The simulation starts from a pure monomer at liquid density (ρ), taken as $0.60\sigma^{-2}$ and $0.80\sigma^{-3}$ in two and three dimensions, respectively. In this system we perform an initiation step, simply by changing the identity of a given, randomly chosen, fraction $\phi_0=[P^*]/\rho$ of the monomer liquid into growth centers. The growth simulation is then performed by successive reaction and dynamic steps, as described before.

All simulations are performed in the $\mathcal{N}VT$-ensemble ($\mathcal{N}$ being the total number of particles) using the Nosé–Hoover technique[32] with a thermostate friction of $0.025\,\tau$ to keep the temperature to a preset value, which was taken to be $1.0\epsilon/k_B$. Throughout this report we use the reduced units ϵ, σ, and $\tau=\sigma(m/\epsilon)^{1/2}$. The mass m is the same for all free monomers and beads. The time step is 0.005τ, which is much smaller than the mean collision time.

We remark that in this model reaction and equilibration take place simultaneously. Hence, the model involves two time scales; the reaction time scale is set by the time between two reaction trials, τ_r. Secondly, the equilibrium motion, including diffusion of free monomers and polymer chains, is set by the temperature, and internal motion of the chains mainly depends on the chain length. In an attempt to discriminate among the time scales we have varied the reaction rate using the parameter τ_r. However, it is obvious that as polymerization proceeds, eventually the relaxation of the chains becomes the slowest process in the system.

III. RESULTS

We are interested in the properties of the chains grown by the proposed method using the system at equilibrium as a reference. To this end we start with calculating the equilibrium properties of our model, in particular the case of a single chain in a solvent (Sec. III A). Here we focus on the static properties as a function of chain length. Next we calculate the same properties from the growth simulations. We investigate the effect of the reaction rate, by varying the time interval between successive reactions, τ_r (Sec. III B). We proceed by extending the growth simulation to simultaneous growth of several chains into the semi-dilute and concentrated regime (Sec. III C). The simulated growth process is compared with the kinetic equations derived in the previous section.

We recall that in our model all interactions are equal; there is no net interaction between polymer segments and solvent molecules and only excluded volume (EV) is operational. The EV severely restricts the volume available to the polymer, so that it spreads over a larger volume and the average size increases with respect to the unperturbed chain, i.e., it swells. On the other hand, EV is also present in the solvent; thus, whereas a polymer swells in the solvent, swelling is less than the swelling of the same chain in a gas or vacuum. We emphasize that, although the solvent may com-

press the chain as density increases, the solvent does not prevent the chain from swelling; as long as the solvent is much smaller than the polymer its effect is essentially that of an external pressure bath. This, of course, cannot hold if the solvent itself is a polymer, i.e., in the case of a polymer melt. Indeed, Flory's hypothesis states just this, that in the melt the chains are not swollen, but behave like if there was no EV.[11]

For sufficiently long chains diluted in a solvent the problem of estimating polymer sizes becomes particularly simple, as it is known to obey a scaling relation[20]

$$X = b_X N^{\nu}, \tag{14}$$

where X stands for any variable characterizing the average size of a chain with $N+1$ monomers and b_X is a model-dependent prefactor with the unit of length; in particular we will focus on the end-to-end distance $X^2 = \langle R^2 \rangle = \langle r_{0N}^2 \rangle$ and the radius of gyration $X^2 = \langle S^2 \rangle = [\,1/(N+1)\,]\,\Sigma_{i,j}\langle r_{ij}^2 \rangle$, where r_{ij} is the distance between bead i and j. The exponent ν is independent of the choice for X and characterizes the scaling regime of an infinitely long chain. In the presence of EV the exponent is equal to $3/(d+2)$ in d-dimensions, according to the standard Flory-argument.[20,33] In the absence of EV the chain is equivalent to a random walk and the corresponding exponent is $\frac{1}{2}$. This indeed shows that chains are swollen by EV interactions, and that this is more pronounced in the lower dimension.

The Flory-argument relies on minimizing an approximated expression for the free energy of the chain, but results in surprisingly accurate values for ν. The values obtained using more sophisticated methods[34] include 0.588 ± 0.001 (using renormalization theory[35]) for $d=3$ and $\frac{3}{4}$ (using Coulomb gas renormalization[36] or conformal group invariance[37]) for $d=2$. These values have also been confirmed by computer simulations[34] and will be used by us in this study.

A. Single chains at equilibrium

We calculated the size of a polymer chain diluted in a solvent of like particles. In order to compare our results with the scaling relation (14), the chain has to be sufficiently long and the concentration has to be sufficiently low. As the simulation box has periodic boundaries we can exclude direct interaction of the chain with any of its periodic images by adding solvent. If we anticipate on the result that due to equilibrium fluctuations chains expand at most twice their average size, for which we substitute a sphere with radius of gyration S, we have the condition $L/S > 4$, where L is the box size in one direction. To exclude hydrodynamic interactions as well, box sizes should be even larger than this. However, we will be concerned with static properties, for which hydrodynamic interactions are found to be of no importance.[38,39]

To estimate the total simulation time that is required to sample the conformational space by time evolution we have to take into account that relaxation times scale with exponent $d\nu$ to the chain length.[33] Thus, sampling the conformations of a $N=100$ chain requires ~ 60 times longer runs than is required for a $N=10$ chain (in three dimensions). This adds to the increase in the total number of particles, which increases with the same exponent (since $\mathcal{N} \propto L^d \propto S^d \propto N^{d\nu}$). As the time spend by the computer is (in the fortunate case) more or less proportional to the number of particles, it increases with an exponent $2d\nu$. To give an indication, for $N=99$ (the longest chain we simulated) in three dimensions it was necessary to simulate 15 000 particles over $100\,000\tau$ (say, ~ 0.2 μs if we substitute the parameters for a typical methylene monomer).

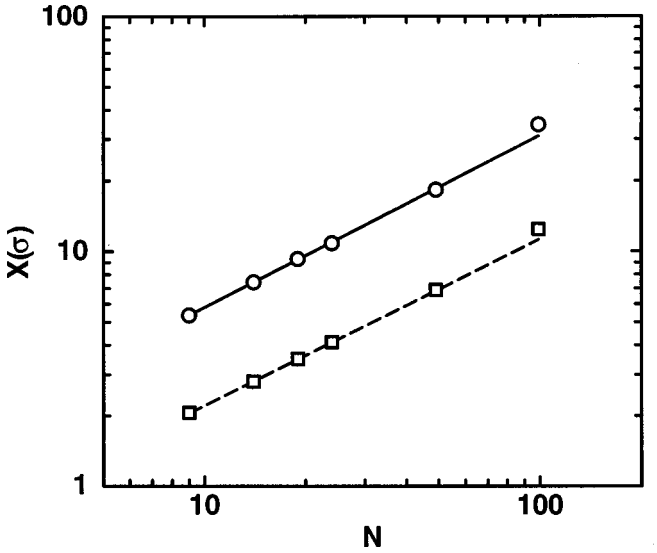

FIG. 1. Root-mean-square end-to-end distances (circles) and radii of gyration (squares) vs the number of bonds N of two-dimensional chains in dilute solution drawn on double logarithmic scale. Also shown are the scaling laws with $\nu = \frac{3}{4}$ and fitted prefactors.

We have calculated the root mean square end-to-end distance and radius of gyration of chains of length from 10 to 100 monomers. Results are shown on log–log format in Figs. 1 and 2 for two- and three-dimensional systems. Also shown are curves with the universal exponents for the EV regime, 0.588 for $d=3$ and $\frac{3}{4}$ for $d=2$. The results are in good

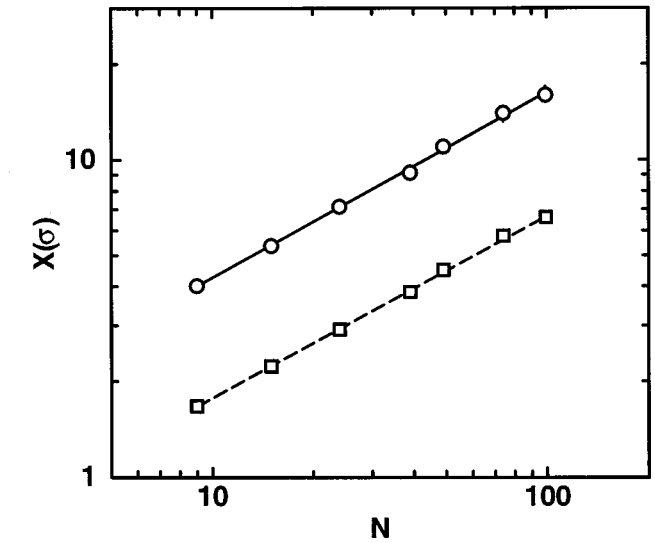

FIG. 2. Root-mean-square end-to-end distances (circles) and radii of gyration (squares) vs the number of bonds N of three-dimensional chains in dilute solution drawn on double logarithmic scale. Also shown are the scaling laws with $\nu = 0.588$ and fitted prefactors.

agreement with the theoretical exponents. The chains are clearly swollen and even the shortest chain ($N=9$) studied is in accordance with the scaling relation.

Using the universal scaling exponents, we calculated the prefactors b_X from Eq. (14), obtaining $b_R=1.0\sigma$ and $b_S=0.38\sigma$ in the limit for long chains in two dimensions. In three dimensions we obtained $b_R=1.15\sigma$ and $b_S=0.45\sigma$. Note that the two factors involve only one model dependent parameter, as their ratio is another universal constant.[34] An approximate value for this ratio can be found by substituting the scaling relation for all segments r_{ij} in the definition of the radius of gyration; this yields $(b_R/b_S)^2=(2\nu+1)(2\nu+2)$ which equals 8.75 ($d=2$) and 6.91 ($d=3$). This should be compared with 6 for a random walk and 12 for a rigid rod. We first note that the characteristic length of the chain is similar to the equilibrium bond length, $b_R \approx r_m$. The radii of gyration are somewhat higher than suggested by the approximation given above; this stems from the fact that internal segments are relatively more swollen than the chain itself. Using direct renormalization one obtains 7.51, respectively, 6.30 as the ratio,[34] whereas the simulation gives us 6.91, respectively, 6.53. The results are in qualitative agreement, but the convergence is rather slow. To account for the difference in swelling between inner segments we probably need much longer chains.

Further evidence for EV behavior is found from all other moments, by investigating the distribution of end-to-end distances. The distribution of $\boldsymbol{R}$ is predicted to scale according to[34]

$$X^d P(\boldsymbol{R}) = f(\boldsymbol{R}/X), \tag{15}$$

where $X=\langle R^2\rangle^{1/2}$ and $f(\boldsymbol{r})$ is a scaling function with zeroth and second moment equal to 1. The asymptotic behavior of f for small and large values of r can be derived using field or renormalization theory[40–42]

$$f(\boldsymbol{r}) \propto \begin{cases} r^{\theta}, & r \ll 1 \\ r^{\kappa} \exp(-Cr^{\delta}), & r \gg 1 \end{cases}, \tag{16}$$

where θ, κ, and δ are universal constants. Note that $P(\boldsymbol{R})$, and consequently also $f(\boldsymbol{r})$, describe the full distribution of the vector $\boldsymbol{R}$. The proportionality constant and C are derived from the unity moments of f. Since θ and κ are predicted to be close in magnitude,[34] it is reasonable to use the second expression for the whole range of r, with κ replaced by θ. Note that for $\theta=0$ and $\delta=2$, $f(\boldsymbol{r})$ is a Gaussian distribution, valid for random walks ($\nu=\frac{1}{2}$). For chains with excluded volume θ must be larger than zero, as $f(\boldsymbol{r})\to 0$ for $r\to 0$. Hence, θ measures the strength of EV interaction at small distances. For infinitely long chains it has been found that $\theta=0.275$.[40,42] The parameter δ describes the tail of the distribution and should be related to ν. Indeed it has been found that $\delta=1/(1-\nu)$,[41] which is also consistent with the random walk case.

The vector distribution of the reduced distance $r=R/X$ is shown in Fig. 3 for different chain lengths in three dimensions. The data reduce reasonably well to a universal distribution. Also shown is the theoretical prediction using $\delta=2.427$ and $\theta=0.275$. The behavior for large r is in accordance with theory, whereas for short distances the theory underestimates the effective excluded volume. This may be due to the finite size of the chains; the reduced range of the excluded volume interaction cannot be neglected in this figure. The effective value of θ should be higher. Using exact enumeration for chains with $N<18$ Domb conjectured[43] $\theta=\delta-2=0.427$. The corresponding distribution is also shown in Fig. 3. Clearly the agreement for small r is improved. However, it has been shown recently[44] that for sufficiently long chains $N>200$ the lower value $\theta=0.275$ is far superior.

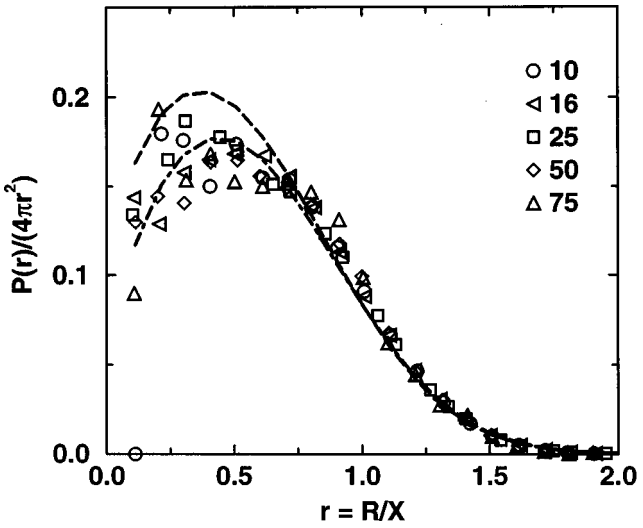

FIG. 3. Distribution of the end-to-end vector $\boldsymbol{R}$ vs the scaled end-to-end distance $r=R/\langle R^2\rangle^{1/2}$ for several chain lengths studied. Also shown is the theoretical curve $f(r)=0.3r^{0.275}\exp(-1.271r^{2.427})$ (upper curve) and the conjecture of Domb (lower curve).

As discussed in Sec. II, the radial distribution function of monomers around a chain end is of interest to estimate the reaction rate coefficient from Eq. (13). The number of free monomers around a chain end depends on the chain length, as neighboring polymer beads prevent monomers from getting close to the chain end. The average number of monomers within a distance r_m from a chain end is shown for different chain lengths in Fig. 4 for both the two- and three-dimensional case. We can see that for any but the shortest chains it approaches an asymptotic value of 0.75 ($d=2$) and 3.4 ($d=3$). The large difference stems not only from the dimensionality but also from the different densities. If we divide the asymptotic values by the monomer concentration, which is essentially the liquid density in this dilute regime, we obtain the integral over $g_{MP*}(r)$ in Eq. (13). Using $m_{\max}=8$ we then find, $k\tau_r=0.16\sigma^2$ and $0.53\sigma^3$ in two and three dimensions, respectively.

Finally, we calculated the diffusion coefficient for the pure monomer liquid, for comparison with the reaction time scale. Using the Einstein relation $D=\langle(\boldsymbol{r}(t)-\boldsymbol{r}(0))^2\rangle^{1/2}/2dt$ we obtain $D=0.25\sigma^2/\tau$ and $D=0.08\sigma^3/\tau$ for two and three dimensions, respectively. Again, the diffusion is faster in two dimensions because of the low density.

B. Single chains growth

We next investigated to what extend the proposed growth mechanism reproduces the properties of a single

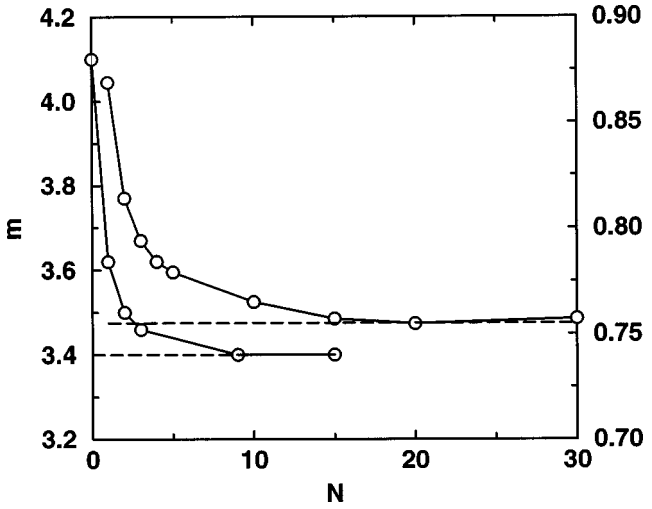

FIG. 4. Average number of monomers m within a distance r_m from a chain end vs chain length in two (right scale) and three dimensions (left scale). The numbers reach asymptotic values indicated by the broken lines.

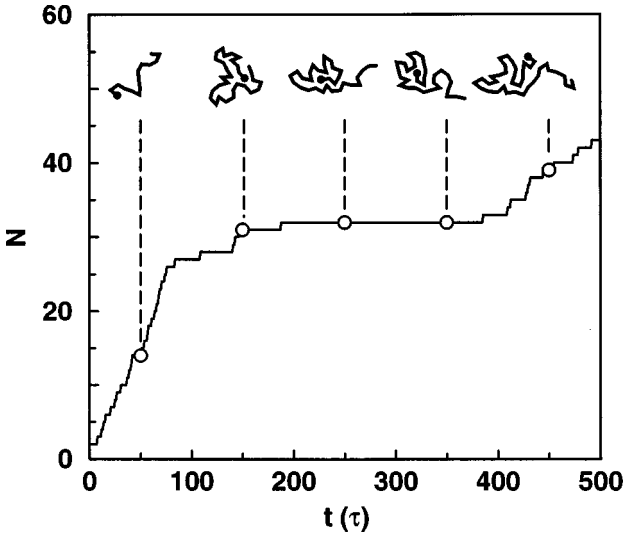

FIG. 5. Growth curve of a single two-dimensional chain in a dilute solution. Each $\tau_r = 1\tau$ a reaction trial is performed. Also shown are snapshots of the growing chain indicating trapping of the growth center.

chain at equilibrium. The kinetics of the growth is parameterized by the time interval between two successive reactions, τ_r. By simple arguments we can speculate on its effect on the polymer properties.

If τ_r is small compared to, say, the time a monomer needs to travel its own diameter, growth is more or less static. That is, we perform a random walk on a frozen disordered lattice, by stepping to free monomers only. If no free monomers are left, the walk stops unless a free monomer moves into the capture radius of the growth center. In the absence of diffusion, this situation is similar to Rosenbluth sampling of self-avoiding walks on a lattice.[45] In this sampling method a walker has some knowledge about its local environment and a next step on such a walk jumps to empty sites only. By stepping to unoccupied sites only, the Rosenbluth sampling favors steps, that eventually lead to compact walks, above excluded sites, whereas *a priori* all directions should be equally probable.[46] We should note that in our growth method we grow only with a probability $m/m_{\max}$, where m is the number of available directions and $m_{\max}$ a fixed number. However, the unreacted chains are not rejected but remain in the system; they are the starting point for the next reaction. These chains are on average more contracted than others (since m is small). Hence, for small τ_r we expect to find an ensemble of configurations that is biased to less swollen chains, with respect to the equilibrium distribution.

On the other hand, if τ_r is sufficiently large, monomers can diffuse in and out the capture radius of the growth center in between two reactive collisions. Any bias introduced by the growing method towards a certain distribution of configurations should become unimportant as the chain has enough time to relax from the nonequilibrium state. However, this relaxation time increases with the chain length. For this reason the process becomes diffusion controlled even for the slowest reaction.

We simulated single chain growth for several reaction intervals ranging from $\tau_r = 0.25$ to 25τ at the same state point as our equilibrium simulations. The total volume was always chosen so as to satisfy $L > 4S$. The simulations were repeated up to 500 times starting from a random growth center in an equilibrated monomer liquid to obtain a reasonable ensemble average. At intervals of τ_r we calculated the number of bonds (N) and sizes (R,S) of the chain.

A typical growth behavior of one chain in a two-dimensional system is shown in Fig. 5. In this case $\tau_r = 1\tau$ and what we see is a succession of successful and unsuccessful reactions. Note that this is only a single experiment; it cannot tell us whether a failed reaction happened by accident or is due to a limited number of reactants. However, the repeated failures in this particular sample indicate that the chain end is trapped in a cage of polymer beads. This is confirmed by the snapshots of the chain, shown in the same figure.

On average over a number of simulations we obtained a smooth curve with decreasing slope, as shown in Fig. 6. Also shown is the curve based on Eq. (10). As the concentration of growth centers is very small, only the term linear in time is important; clearly, the consumption of monomer is not the reason for the decreasing growth rate. Instead, the decrease is due to two effects. First, at some stage the reactive site becomes trapped. The trapping probability increases in time because the polymer concentration around the chain end increases, as was shown in Fig. 4 for a chain in equilibrium. Also, in our growth method the chain tends to grow into compact conformations, making trapping more likely.

Second, if the chain end is trapped, growth can only proceed after the growth center has diffused back into the monomer phase or when the monomers have diffused towards the growth center. The diffusion of free monomers from the bulk to the trapped growth center is hindered by the polymer beads in the coil, and this process will slow down as the coil volume increases. At the same time the polymer relaxation slows down with increasing chain length. Hence, the time that is needed to recover from a trapped situation increases in time.

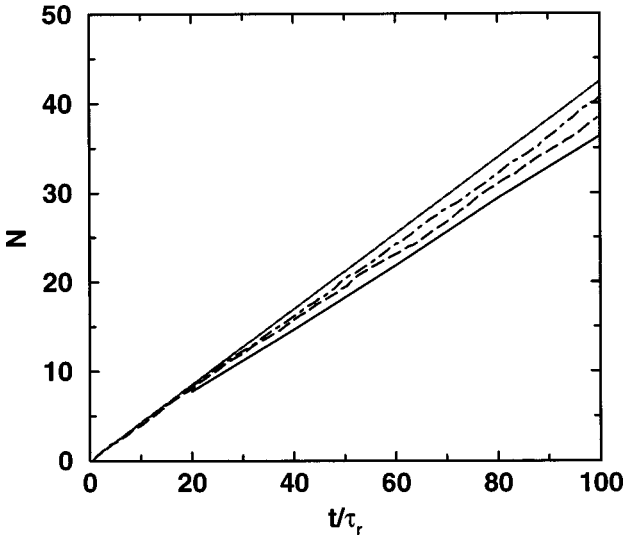

FIG. 6. Growth curve of a three-dimensional chain grown in a dilute solution. Results for three different reaction rates are shown: $\tau_r=0.05\tau$ (solid), $\tau_r=0.5\tau$ (dashed) and $\tau_r=25\tau$ (dot–dashed). The upper straight solid line corresponds to $N=k[M]_0t$ where the rate constant k is calculated from Eq. (13).

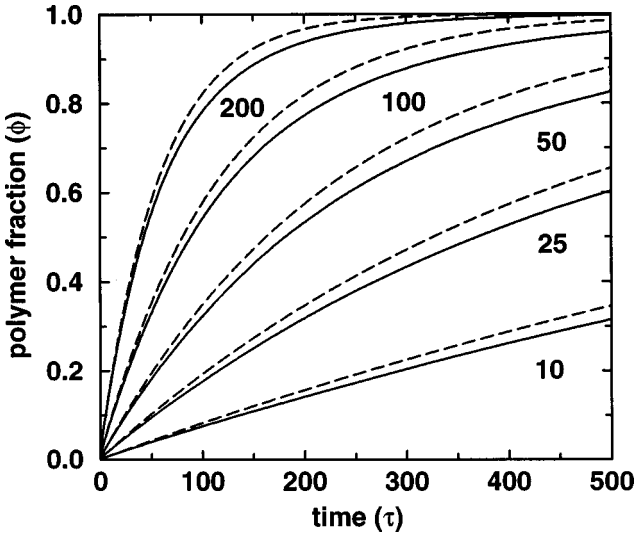

FIG. 8. Polymer fraction in time for different number of growth centers as indicated in the figure (total number of particles $\mathcal{N}=10\,000$) from simulation (solid) and theory (dashed) in three dimensions. The reaction interval τ_r is equal to 0.5 τ.

Average growth curves are shown for several reaction intervals in Fig. 6 for growth in three dimensions. We see that for the fastest reaction, diffusion is important already after a few reaction steps, whereas the slowest reaction follows the kinetics much longer. However, even the slowest reaction is limited by diffusion on the MD time scale. Clearly the reaction rates should be much smaller to discriminate amongst the reaction and diffusion time scales.

The end-to-end distances and radii of gyration are shown versus chain length for two different reaction rates in Fig. 7. Also shown are the scaling results using the prefactors obtained from the equilibrium simulations. The results of the fastest reaction ($\tau_r=0.05\tau$) are averaged over 500 simulations, whereas for the slowest reaction ($\tau_r=25\tau$) we used 100 simulations. Note that the reaction rates differ a factor of 500; in the slowest case, each simulation takes about 5 ns, after substituting the parameters for a typical methylene unit. Although results suffer from statistical error due to the finite ensemble, they indicate that the rapidly grown chains are less swollen with respect to the equilibrium chains. This ''effective attraction'' is due to the growth method and is similar to the Rosenbluth bias in sampling self-avoiding walks. The slowest reaction is already in good correspondence with the equilibrium results.

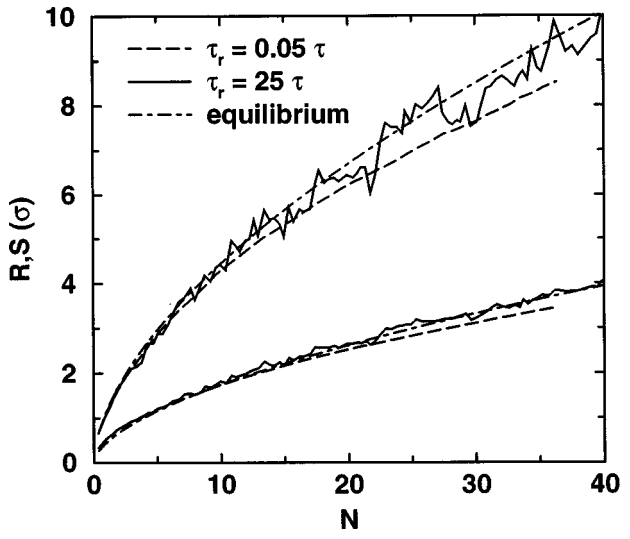

FIG. 7. Average radius of gyration (lower curves) and end-to-end distance (upper curves) vs chain length of a three-dimensional chain grown in a dilute solution for a slow ($\tau_r=25\tau$) and a fast ($\tau_r=0.05\tau$) reaction. Also shown is the scaling law with $\nu=0.588$ and the prefactors obtained from equilibrium simulations.

C. Multiple chains growth

We also studied the simultaneous growth of several chains. Here, we start from a dilute system as before and follow growth to the stage where chains start to interact and further, until we reach the concentrated regime and, finally, the polymer melt.

As before we start from a monomer liquid ($\mathcal{N}=10\,000$) at the same thermodynamic point as before with a small fraction ($\phi_0=[P^*]/\rho$) of growth centers randomly distributed in the liquid. Growth simulations were then performed for various reaction rates each repeated 50–500 times, starting from different initial states.

The average growth behavior is shown in Fig. 8 for a three-dimensional system using several concentrations of initiator, $\phi_0=0.001$–0.02. Also shown are the curves based on Eq. (10) using the value for the reaction rate coefficient obtained from Eq. (13), $k\tau_r=0.53\sigma^3$. In these simulations we applied $\tau_r=0.5\tau$, hence $k=1.06\sigma^3/\tau$. According to Eq. (10) the chain length grows linearly in time and then levels off exponentially to its asymptotic maximum. A fully converted system is not obtained on the MD time scale, as small clusters of reactants are left and they diffuse only slowly to the growth centers. Although the kinetic model overestimates the polymer production the shape is very well represented.

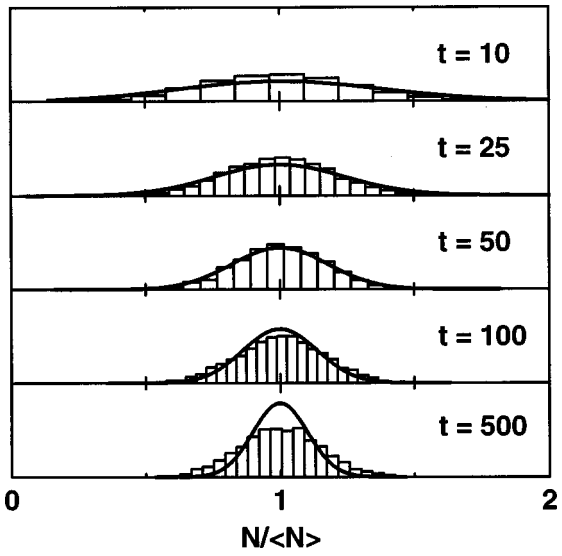

FIG. 9. Molecular weight distribution for different time as indicated in the figure in reduced units for $\phi_0=0.1$ and $\tau_r=0.5\tau$ from simulations (histogram) and theory (solid line).

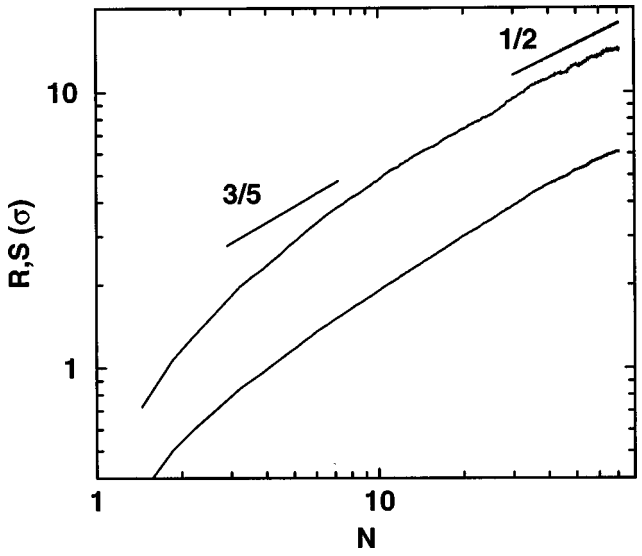

FIG. 10. Root-mean-square end-to-end distance (upper curve) and radius of gyration (lower curve) vs chain length measured during the growth in three dimensions drawn on double logarithmic scale. A crossover is observed from excluded-volume behavior ($\nu=0.588$) to Gaussian behavior ($\nu=\frac{1}{2}$).

Indeed, good agreement is found for all initiator concentrations using an effective, lower, value for $k\approx 0.95\sigma^3/\tau$.

Apart from the average chain length, one is often interested in the dispersity, or shape of the molecular weight distribution. In Fig. 9 we show the distribution of chain sizes reduced on the mean, for different times during the growth process. As expected the distribution becomes more peaked around its mean value as polymerization increases. This is a consequence of the absence of termination processes; all chains keep on growing as long as there are reactants left. Also shown in Fig. 9 are curves predicted by Eq. (12) using an effective value for the reaction rate constant, $k=0.95\sigma^3/\tau$. We see that the shape of the theoretical distribution is reasonably well reproduced. Near completion of the reaction, diffusion controls the growth process as the fraction of reactants is very low. The predicted distributions are therefore too narrow with respect to the simulation results.

We also followed the chain size during the growth. The end-to-end distance and radius of gyration of the chains during the polymerization are shown in Fig. 10 for the three dimensional case. We observe two scaling regimes. In the first stage the chains grow into swollen conformations, just as we saw for growth of a single chain. Then, as polymerization proceeds, chains start to interact and the swollen conformations are compressed by these interactions. Finally the interchain interactions more or less offset the intrachain interactions, and we end up with random walk statistics and the corresponding scaling exponent $\nu=\frac{1}{2}$.

It would be interesting to know if we can predict the concentration separating the regimes of detached and overlapped chains. Clearly, this is not a sharp transition, but rather an average concentration around which interchain interactions are getting important. A simple estimate stems from the idea that at the crossover point the concentration inside the swollen coil is equal to the overall concentration.[20] That is, the solution is densely packed with swollen coils. If we take the coil to be a sphere with radius of gyration and apply the scaling relation (14), we find

$$N\phi_0\rho/\eta_d=\frac{N\Gamma(d/2+1)}{\pi^{d/2}S^d}=\frac{N\Gamma(d/2+1)}{\pi^{d/2}b_S^dN^{\nu d}}\,, \tag{17}$$

where η_d stands for the maximum packing fraction in d dimensions. Using Flory's approximation to ν

$$N=\left(\left(\frac{\Gamma(d/2+1)\,\eta_d}{\pi^{d/2}}\right)\rho b_S^d\phi_0\right)^{(2+d)/3d}\,, \tag{18}$$

in which the fraction inside the brackets equals 1/4 and $1/\sqrt{32}$ for $d=2$ and 3, respectively.

From the simulation we estimate the crossover point by extrapolating from the two scaling regimes. We define the crossover point by the point at which the two extrapolations cross. The crossover concentrations obtained this way are shown in Fig. 11, together with the estimate using Eq. (18). Here we used the two-dimensional system as in two dimensions the difference between a swollen and screened chain is more pronounced.

The chains start to contract much before the predicted crossover points. This is not surprising as at the predicted critical concentrations all chains already strongly interact, though not interpenetrate. Furthermore, our solution is polydisperse and the chains are not spherical in shape. The latter was revealed by calculating the eigenvalues of the inertia tensor, which shows that the chains are rather ellipsoidal ($\lambda_{\max}\approx 0.9S^2$) and thus sweep out a much larger volume.

In order to get a better description we applied another criterium that does not depend on these two effects. At the crossover point chains start to interact, and if all chains interact with one another we could think of a percolating polymer phase. This approach is somehow similar to the excimer fluorescence measurements which are used to reveal the transition.[47] There one measures the fluorescence intensities

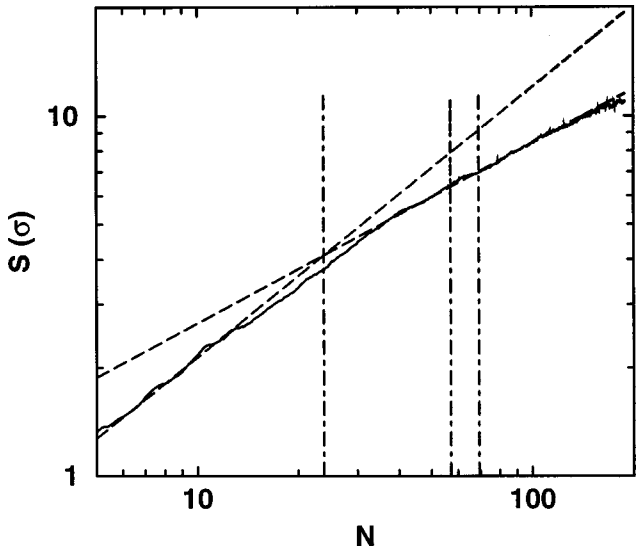

FIG. 11. Root-mean-square radius of gyration vs chain length of a two-dimensional polymer measured during a growth process with $\phi_0=0.05$. Also shown are the two scaling laws ($\nu=\frac{3}{4}$ and $\frac{1}{2}$) and their crossing at $N\approx 23$. The second line at $N\approx 53$ corresponds to the percolation threshold and the third line at $N\approx 70$ corresponds to the crossover points according to Eq. (18).

due to excimer formation with respect to the monomer fluorescence. This ratio starts to grow in the vicinity of the crossover, as excimers are formed between chromophores on different chains.

We calculated the cluster distribution during the growth process and determined the instant at which there is for the first time only a single cluster of polymer beads in the system. The critical distance within which two beads are said to be clustered is chosen to be equal to the position of the first minimum of the radial distribution function, $r=1.75$ for $d=2$. The corresponding concentration is also shown in Fig. 11 and agrees somewhat better with the simulated data. Still, the chains are already screened at the moment the system percolates for the first time.

We conclude that both the percolation and the packed blobs picture of the crossover state predict concentrations that correspond to screened chains in our simulations. The crossover point that we find from our simulations corresponds to a diluted system in which only a fraction of the coils interact.

The structure of the growing system was investigated by calculating the structure factor $S(k)$ for different wave vectors $\boldsymbol{k}$

$$\mathcal{N}S(k)=\langle\hat{\rho}(\boldsymbol{k})\hat{\rho}(-\boldsymbol{k})\rangle, \tag{19}$$

where $\hat{\rho}(\boldsymbol{k})$ is the Fourier-transform of the instantaneous density $\rho(\boldsymbol{r})$

$$\hat{\rho}(\boldsymbol{k})=\int \exp(i\boldsymbol{k}\cdot\boldsymbol{r})\rho(\boldsymbol{r})d\boldsymbol{r}=\sum_{j=1}^{\mathcal{N}} \exp(i\boldsymbol{k}\cdot\boldsymbol{r}_j), \tag{20}$$

with $\boldsymbol{r}_j$ the coordinate of particle j and $\mathcal{N}$ denotes the number of scattering centers. To obtain the structure factor, we mapped the density in continuous space on a grid. The discrete density was then Fourier-transformed to a d-dimensional grid in the reciprocal space. The transformed density was correlated and circular averaged to obtain $S(k)$, assuming spherical symmetry.

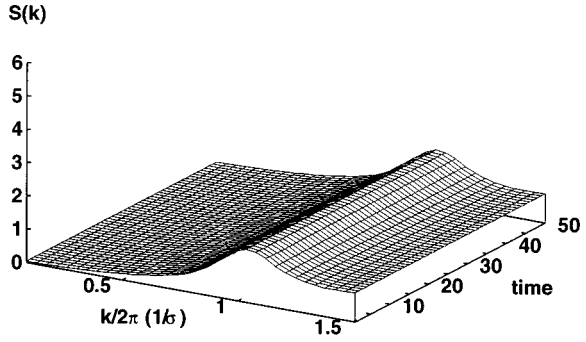

FIG. 12. Total structure factor starting from a monomer liquid at $t=0$ and evolving to a polymer melt. Each 0.5τ a reaction trial was performed.

We first calculated the structure factor by taking all particles into account. This total structure factor $S(k)$ is shown in Fig. 12 for different stages of the growth process, starting from a monomer liquid at $t=0$ and ending with a polymer melt at $t\approx 50\tau$. Interestingly, it does not change significantly during the process; that is, the fluid structure is maintained also in the melt. The strong intensity at $k\sim 2\pi\sigma^{-1}$ represents the first neighbors of the particle. As we have set the equilibrium bond length to the Lennard-Jones minimum (r_m), the same wavelength also probes the bonded neighbors. Also the behavior for $k\rightarrow 0$ is very much the same. In other words, the compressibility of the monomer liquid is similar to that of the melt. We should note, however, that we observe a drop in the pressure as growth proceeds. Apparently, the effect is too small to affect the total structure factor.

We further calculated the structure factor taking only the polymer or solvent particles as scattering centers. The polymer structure factor, S_{PP} is shown in Fig. 13. Initially it is unity, since the growth centers are randomly distributed in the system. Then, bonds are created and the intensity increases for $k\sim 2\pi/r_m$. At the same time the intensity increases for small values of k ($k\lesssim 0.1$ rad/σ). This small k behavior for short times shows that polymer beads are grown locally at the growth centers; that is, in the dilute regime the polymer material is clustered as small islands. Taking the

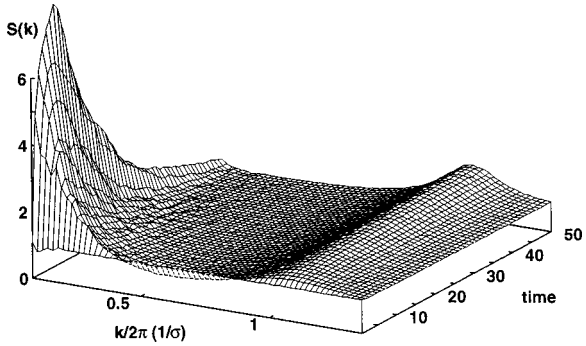

FIG. 13. Structure factor of the polymer particles starting from a monomer liquid at $t=0$ and evolving to a polymer melt. Each 0.5τ a reaction trial was performed.

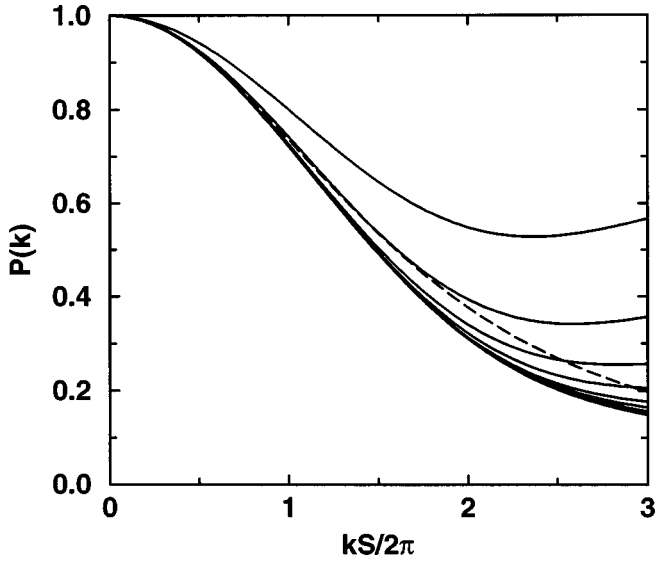

FIG. 14. Form factor of the polymer chains vs the wavelength reduced by the radius of gyration in three dimensions for various stages of the process, $t=1,2,\ldots,15\tau$ from top to bottom. The initial polymer fraction is 0.01 and each 0.5τ a reaction trial was performed. Also shown is the Debye function for Gaussian chains (dashed).

homogeneous distribution as a reference, this corresponds to a large density fluctuation and hence $S_{PP}(k\rightarrow 0)$ increases. This strong intensity then decreases as growth proceeds and the polymer phase approaches a homogeneous distribution. This reduction of intensity is due to correlation between beads on different chains. We could therefore relate the maximum in $S_{PP}(k\rightarrow 0)$ to the onset of the crossover region in Fig. 11. Finally, we obtain almost the same structure factor as found for the solvent.

We have investigated the polymer structure factor into more detail by discern interference due to correlation of scattering centers within a single chain and of scattering centers on different molecules. The former is represented by the form factor $P(k)$

$$N^2P(k)=\left\langle \sum_{j=0}^{N}\sum_{l=0}^{N} \exp(i\mathbf{k}\cdot(\mathbf{r}_j-\mathbf{r}_l))\right\rangle = \left\langle \sum_{j=0}^{N}\sum_{l=0}^{N} \frac{\sin(kr_{jl})}{kr_{jl}}\right\rangle, \tag{21}$$

where r_{jl} is the distance between two beads on a single chain with N bonds. The last equation is valid in three dimensions, by explicitly assuming spherical symmetry. Expanding Eq. (21) for small k shows that the form factor is proportional to the radius of gyration times k^2. We have shown the form factor for different times ($t=1,2,\ldots,15\tau$) in Fig. 14 reducing the scattering vector by the radius of gyration. Apart from the very beginning the form factor is seen to obey the suggested scaling for all wavelengths. Also shown is the structure factor for a Gaussian chain[33]

$$P(k)=2(\exp(-x)+x-1)/x^2, \quad x=k^2S^2. \tag{22}$$

This so-called Debye expression is in reasonable agreement with the structure at small k, but overestimates the intensity at high k. Thus, although the scaling of the radius of gyration suggests screening of interactions and hence Gaussian behavior, on sufficiently small length scales this simple picture breaks down.

IV. CONCLUSIONS

In this work we have presented a simple model to simulate polymerization processes by means of molecular-dynamics simulation. In the growth method, reaction, and equilibration take place simultaneously. We applied the growth method to a bead-spring model and find that it produces polymer melt samples in accordance with the expected equilibrium distribution. That is, for sufficiently slow reactions the chains grow as swollen chains in the diluted regime, with properties in accordance with the system in equilibrium. As concentration increases, the chains start to interact and become screened, which results in Gaussian chain statistics.

We have compared the simulation results with a kinetic scheme. The latter is based on the assumption there is ideal mixing and no limitation due to diffusion. In the case of a single chain we found that it describes the first stage of the process quite well. However, growth centers can easily become trapped in a cage of polymer beads, especially in two dimensions. In such cases diffusion of reactants towards the growth center controls the process, because the reaction rate is fast compared to diffusion. This means that the kinetic model predicts too fast growth.

It was also found that if the reaction is fast, not only diffusion processes become important, but the properties of the chains differed from those generated by a slow polymerization. By examining the growth model we argued that this is similar to the Rosenbluth bias, which one finds, for example, in sampling the properties of a self-avoiding walk. However, even with the range of reaction rates accessible to the MD time scale it is possible to choose a reaction rate that is sufficiently slow such that all memory of the growth method is lost within two reactions and equilibrium properties are obtained.

The growth simulations of multiple chains again showed the effect of diffusion limitation. The predicted conversions were somewhat too high, but this can be accounted for by choosing an effective rate constant. Using this effective value, we saw that also all other moments of the molecular weight distribution are in agreement with the predicted Poisson distribution.

Although in this work we have primarily been concerned with studying the growth process in time, as pointed out in the introduction, the technique may be used to generate polymer–solvent structures as starting configurations in MD simulations. An important question is what is the efficiency as compared to existing methods applying the same technique. Based on our investigations we can conclude that a fast growth (say, $k\approx 10\sigma^3/\tau$) yields chains that are on average too contracted in the dilute regime. However, if one is interested in melts this may not be a problem as the chains have to contract to screened conformations anyway. A more relevant side effect is that using these fast reactions, diffusion limitation plays an important role; if the reaction is fast, large clusters of monomers are left unreacted, and the system grows very inhomogeneously. It was found that using k

$\approx 1\sigma^3/\tau$ a reasonably homogeneous system is obtained with conformation statistics that satisfy the equilibrium distribution.

ACKNOWLEDGMENT

Reinier Akkermans acknowledges financial support from the Danish Rectors Conference.

[1] D. N. Theodorou and U. W. Suter, Macromolecules **18**, 1467 (1985).
[2] D. Brown, J. H. R. Clarke, M. Okuda, and T. Yamazaki, J. Chem. Phys. **100**, 6011 (1994).
[3] J. I. McKechnie, D. Brown, and J. H. R. Clarke, Macromolecules **25**, 1562 (1992).
[4] D. Rigby and R.-J. Roe, J. Chem. Phys. **87**, 7285 (1987).
[5] R. Khare, M. E. Paulaitis, and S. R. Lustig, Macromolecules **26**, 7203 (1993).
[6] J. Gao, J. Chem. Phys. **102**, 1074 (1995).
[7] A. Kolinski, J. Skolnick, and R. Yaris, J. Chem. Phys. **84**, 1922 (1986).
[8] M. Kotelyanskii, N. J. Wagner, and M. E. Paulaitis, Macromolecules **29**, 8497 (1996).
[9] S. Gupta, G. B. Westermann-Clark, and I. Bitsanis, J. Chem. Phys. **98**, 634 (1993).
[10] B. Lin, P. T. Boinske, and J. W. Halley, J. Chem. Phys. **105**, 1668 (1996).
[11] P. J. Flory, *Statistical Mechanics of Polymers* (Wiley, New York, 1969).
[12] N. F. A. van der Vegt, W. J. Briels, M. Wessling, and H. Strathmann, J. Chem. Phys. **105**, 8849 (1996).
[13] R. Sok and H. J. C. Berendsen, J. Chem. Phys. **96**, 4699 (1992).
[14] S. Toxvaerd, Phys. Rev. E **53**, 3710 (1996).
[15] *Kinetics of Aggregation and Gelation*, edited by F. Family and D. P. Landau (North-Holland, Amsterdam, 1984).
[16] H. J. Herrmann, D. Stauffer, and D. P. Landau, J. Phys. A **16**, 1221 (1983).
[17] R. Jullien and R. Botet, *Aggregation and Fractal Aggregates* (World Scientific, Singapore, 1987).
[18] T. A. Witten and L. M. Sander, Phys. Rev. B **27**, 5686 (1983).
[19] U. S. Agarwal and D. V. Khakhar, J. Chem. Phys. **99**, 3067 (1993).
[20] P.-G. de Gennes, *Scaling Concepts in Polymer Physics* (Cornell University Press, Ithaca, 1979).
[21] I. Carmesin and K. Kremer, J. Phys. (France) **51**, 915 (1990).
[22] R. Merkel, J. Simon, H. Ringsdorf, and E. Sackman, J. Phys. II **4**, 703 (1994).
[23] H. Meier, I. Sprenger, M. Bärmann, and E. Sackmann, Macromolecules **27**, 7581 (1994).
[24] D. Lefevre, F. Porteu, P. Balog, M. Roulliay, G. Zalczer, and S. Palacin, Langmuir **9**, 150 (1993).
[25] P. Clapp, B. A. Armitage, and D. F. O'Brien, Macromolecules **30**, 32 (1997).
[26] A. Raudino, J. Polym. Sci., Part B: Polym. Phys. **32**, 2311 (1994).
[27] M. R. Riley, H. M. Buettner, F. J. Muzzio, and S. C. Reyes, Biophys. J. **68**, 1716 (1995).
[28] M. Bishop and J. P. J. Michels, J. Chem. Phys. **85**, 1074 (1986).
[29] M. Szwarc and M. van Beylen, *Ionic Polymerization and Living Polymers* (Chapmann & Hall, New York, 1993).
[30] P. J. Flory, *Principles of Polymer Chemistry* (Cornell University Press, New York, 1953).
[31] P. E. M. Allen and C. R. Patrick, *Kinetics and Mechanisms of Polymerization Reactions* (Ellis Horwood, Chichester, 1974).
[32] S. Toxvaerd, Mol. Phys. **72**, 159 (1991).
[33] M. Doi and S. F. Edwards, *The Theory of Polymer Dynamics* (Clarendon, Oxford, 1986).
[34] J. des Cloiseaux and G. Jannink, *Polymers in Solution; Their Modelling and Structure* (Clarendon, Oxford, 1990).
[35] J. C. le Guillou and J. Zinn-Justin, Phys. Rev. Lett. **39**, 95 (1977).
[36] B. Nienhuis, Phys. Rev. Lett. **49**, 1062 (1982).
[37] A. A. Belavin, A. M. Polyakov, and A. B. Zamolodchikov, J. Stat. Phys. **34**, 763 (1984).
[38] C. Pierleoni and J. P. Ryckaert, J. Chem. Phys. **96**, 8539 (1992).
[39] B. Dünweg and K. Kremer, J. Chem. Phys. **99**, 6983 (1993).
[40] J. des Cloiseaux, Phys. Rev. A **10**, 1665 (1974).
[41] M. E. Fischer, J. Chem. Phys. **44**, 661 (1966).
[42] D. McKenzie and M. A. Moore, J. Phys. A **4**, L82 (1971).
[43] J. Gilles, C. Domb, and G. Wilmers, Proc. Phys. Soc. London **85**, 625 (1965).
[44] J. P. Valleau, J. Chem. Phys. **104**, 3071 (1996).
[45] M. Rosenbluth and A. Rosenbluth, J. Chem. Phys. **23**, 356 (1955).
[46] J. Batoulis and K. Kremer, J. Phys. A **21**, 127 (1988).
[47] J. Roots and B. Nyström, Eur. Polym. J. **15**, 1127 (1979).